academic publishers
INTERNATIONAL JOURNAL OF ARTIFICIAL INTELLIGENCE (ISSN: 2692-5206)
Volume 04, Issue 07, 2024
Published Date: 04-10-2024

CONTROLLING THE DISTANCE BETWEEN A MEDICAL ULTRASOUND ROBOT AND AN OBJECT

Nodirbek Ruziyev
Doctoral student of Andijan Mechanical Engineering Institute
Email:nadirbek.roziyev@mail.ru, phone: +998942121448

Abstract. The main reason for the use of robotic ultrasound is to increase the accuracy and consistency of ultrasound examination. By removing the human factor in the inspection process, robotic systems can perform ultrasounds with a level of accuracy that is difficult to achieve manually. This leads to more accurate diagnoses and treatment plans for patients. This article presents the research and development trends of the ultrasonic medical robot.
Keywords.robot systems, ultrasound diagnostic device, intelligent medical robot, control algorithm, control software

1. Introduction

Ultrasound imaging is a universal and widely used clinical detection method in preoperative examinations, characterized by real-time imaging, non-invasiveness, ionizing radiation and lower cost; therefore, this medical imaging equipment is widely used in medical facilities. However, although the ultrasound imaging system has a very high clinical usage rate, it mainly relies on the work experience of doctors. In addition, repeated force application at certain angles is required during the detection process to obtain accurate ultrasound images [1]. In the process of scanning the probe of traditional ultrasound detection, the doctor must hold the probe for a long time with a constant force and a specific angle. Thus, hand shake can occur, leading to unclear images and long-term occupational injury, such as shoulder pain [2]. Currently, an integrated program based on a robotic ultrasound system is suitable to improve the above problems. The robotic system has clear advantages (stability, high success rate, repeatability, dexterity and workability). Thus, the performance of the robotic ultrasound system in image acquisition and control can be effectively improved, which improves the performance of ultrasound image recognition [3,4]. In addition, in recent years, various robotic arms combined with real-time ultrasound imaging have been widely used by various departments for preoperative and intraoperative examinations, and the robotic arms have high stability and system repeatability. due to this, human errors have been significantly reduced [5,6].

The pose of the ultrasound probe in the ultrasound robot refers to its location and orientation relative to the patient or imaged object. Proper control of probe position is essential for obtaining high-quality images and accurate diagnosis. The position of the probe is usually determined using Cartesian coordinates (X, Y, Z) in three-dimensional space. These angles determine the orientation of the probe. Roll refers to tilt left or right, step to move up or down, and spin around a vertical axis. The design of the probe's end effector should provide flexible orientation to access different anatomical areas. Algorithms are used to calculate the necessary movements of the robot's joints to achieve the desired probe pose. Feedback systems can adjust probe position and orientation based on real-time imaging data. It is used for live imaging data to dynamically refine the position of the probe, ensuring optimal contact with the skin and alignment with anatomical structures. An intuitive interface helps operators adjust the position and orientation of the probe during imaging. Additional sensors (such as cameras or laser rangefinders) can be used to ensure accurate probe location and orientation. Regular calibration of the robotic system and probe is essential to maintain

accuracy over time. Providing clinicians with a way to manually adjust the position of the probe can increase flexibility and sensitivity during examinations. Includes training tools to help operators familiarize themselves with probe placement and optimal imaging techniques.

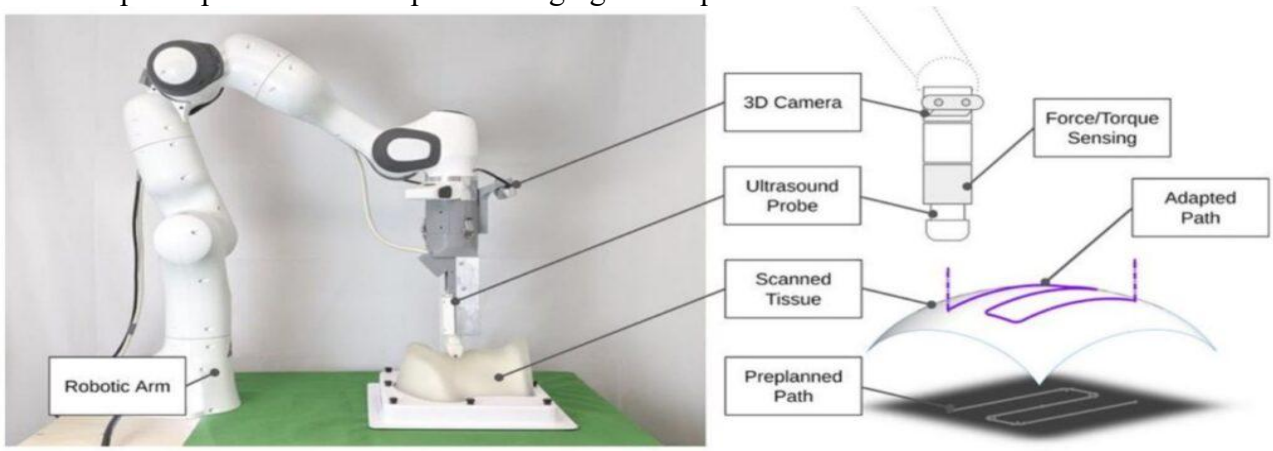

Figure 1: Path inspection of the ultrasound robot

To test the method in a phantom experiment, it can use a 5 mm spacer to simulate the usage scenarios of the probe angles with and without deviation. In each experiment, the ultrasonic arm integrated with the ultrasonic probe armature mechanism starts from its initial position and executes a fixed path program. The program was able to reach the position of the tumor at a 45-degree angle in the simulated liver and scan continuously for 10 seconds with a firm force in this position. In addition to real-time imaging, the robotic ultrasound system recorded and analyzed relevant values.

2. Materials and methods

The architecture of this system was comprised of three items, the six-axis robot arm system, an ultrasound imaging system, and an adjustable fixture mechanism design, as shown in Figure 1. As the six-axis robot arm used in this study was driven by six motors in different positions, each motor could provide uniaxial rotary motions. In terms of the DOF, the six-axis robot arm satisfied the six DOF in a 3D space, which was sufficient for conventional ultrasonic scanning. The ultrasound imaging system used the T-3300 for scanning developed by BenQ Medical. In addition to a sharp image quality, through integration with a robot arm, the system featured high mobility and digital intelligent management. Integrated with a touch screen, the supports intelligentized the gesture operation for lightness, flexibility, and fast booting. It was also highly flexible in an emergency and appropriate for serious symptom examinations for home care. Finally, in order to maintain a stable movement of the ultrasonic probe and force at a specific angle, the adjustable fixture mechanism was integrated with thin film pressure sensor and IMU, meaning the errors were compared for the angle of the ultrasonic probe and the applied force was measured instantly in the automatic scanning process. When the ultrasonic probe shaked during scanning, it led to angle errors. Thus, when the force applied by the robot arm was insufficient, feedback of real-time data analysis was provided, and the robot arm performed real-time angle or force compensation to avoid the preset angle being nonsynchronous with the actual measurement angle. With this architecture, the system could upgrade the quality of the ultrasonic images. To make the different robot arm models compatible with the ultrasonic probe, the system uses an adjustable fixture mechanism, VGA, and an HDMI image capture card to capture ultrasonic images per second. In the analysis process, the motion of the robot arms, the image obtained in the scanning process, and information were transferred to the back-end analytic system synchronously, which provides medical care personnel with a reference for each examination.

The overall workflow of the system is shown in Figure 2. represents the expected reference position, is the expected position sent to the robotic, represents the actual position, and is the position change value of the probe in the vertical direction. represents the external contact force applied to the probe, represents the desired force, and is the difference between them. represents the joint angle of the robot. When the system operates, the point cloud information of the lesion area is first collected using an RGB-D camera. Then, the probe position is automatically outputted

by point cloud processing and path planning. A point cloud normal vector finding framework is established to control the vertical direction of the US probe to ensure that it is perpendicular to the skin surface during the US scanning process. Trajectory planning is then performed for the path points, and the robot's inner loop controller executes the scanning task. The system can control the probe to fit the skin surface for scanning and adjust the contact force in real time according to the feedback.

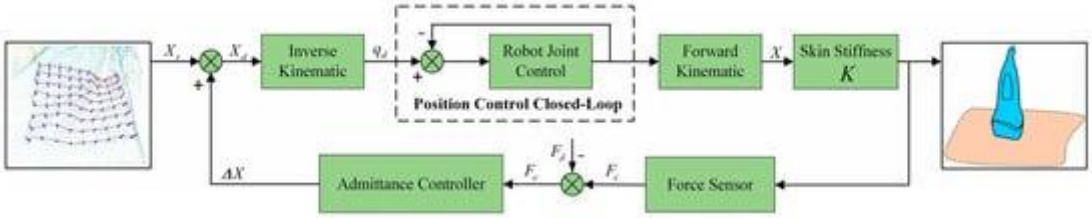

Figure 2. The overall workflow of the system.

To obtain the real contact force, a gravity compensation process based on the raw force data of the autonomous robotic US scanning system is performed. The coordinate system used in this study is shown in Figure 3, where the effect of the inertial forces can be disregarded because of the low speed of the robotic US system.

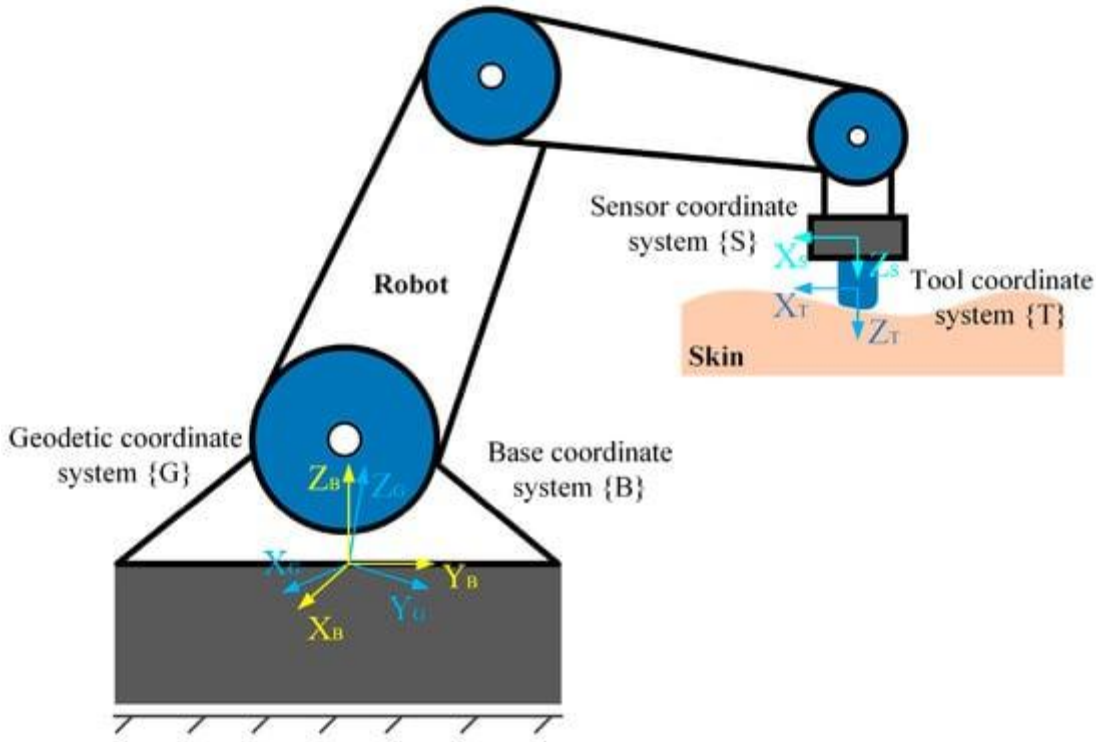

Figure 3. The diagram of the coordinate frames.

To obtain reliable US images, it is necessary to keep the normal direction of the probe coinciding with the normal direction of the skin contact surface during the robotic US scanning process, while the human skin is irregularly curved. Therefore, the robot must adjust its attitude, resulting in a change in the probe gravity in { } . In addition, owing to the sensor's phenomenon of zero drift, it is necessary to determine the actual zero value of the sensor. In this study, we collected 16 sets of sensor data under the general attitude of the robot and used the least squares method to obtain the sensor zero-point, robot mounting inclination, load gravity, and centre of mass simultaneously, thereby eliminating the influences of the sensor zero-point and load gravity on the force perception, and accurately obtained the real contact force and torque data.

3. Simulation results

Simulation experiments were conducted to test and compare three controls, namely AC, IAC, and IAAC, across various environments. Tissues in various parts of the human body exhibit different shapes. For instance, the abdomen and back are relatively flat, while the chest and spine are more complex. Therefore, to test the performance of the proposed control strategy, three representative scenes (flat surface, slope surface, and sine surface) are selected for the experiment. The simulation, executed in

MATLAB/Simulink, includes components like the admittance model, adaptive and integral controllers, robot motion servo system, and environmental dynamics model, as shown in **Figure 3**. The sample time =2 ms =2 ms and admittance parameters are selected. The simulation does not consider any interference. The simulation analysis results are as follows.

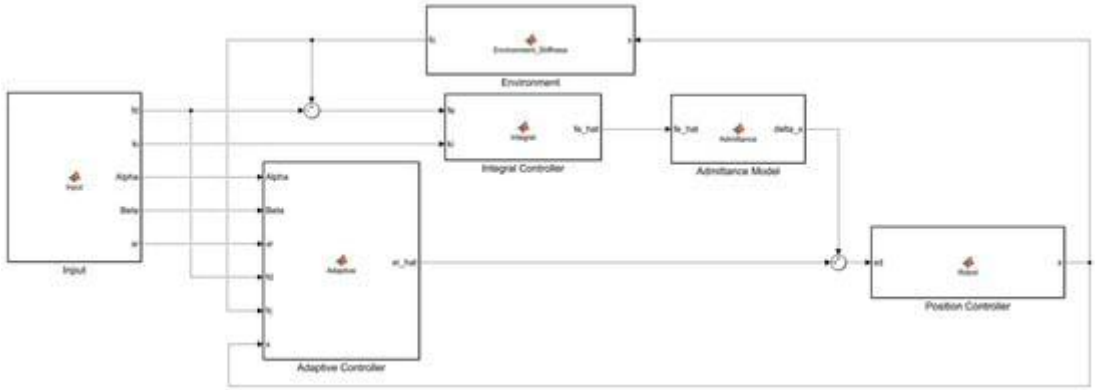

Figure 4. The block diagram of simulation.

The pressure sensor used in this study was GD10-20N developed by Uneo Inc. Thesensor was fabricated using a piezoresistive polymer composite and screen printing as shown in Figure 3. Prior studies have described the typical process method for force-sensing film. First, the electrode pattern and signal transmission line were printed on the substrate. In the course of production, the signal line was wrapped in the insulating layer to avoid signal transmission interference. As GD10-20N was produced using an imprinting and Flexible Printed Circuit (FPC) technique, the line spacing in the insulating layer was 0.1 mm. Thus, a precise circuit could be designed in a micro shape, and fabrication could be customized according to client-side requirements. GD10-20N, which was characterized by lightness, flexibility, and compactness, has good environment fitness, and remains sensitive at harsh ambient temperatures (40_~65 _C). The output of sensors could be adjusted by an amplifier circuit to provide higher voltage range and the resolution. It could increase the correlation between the output and the Newton force (0 N~20 N), which achieved the linearity of regressive analysis to 99%. The sensors could be reused ten million times. According to prior studies, the thin film pressure sensor has the advantages of system integration, as well as data linearity and reliability .

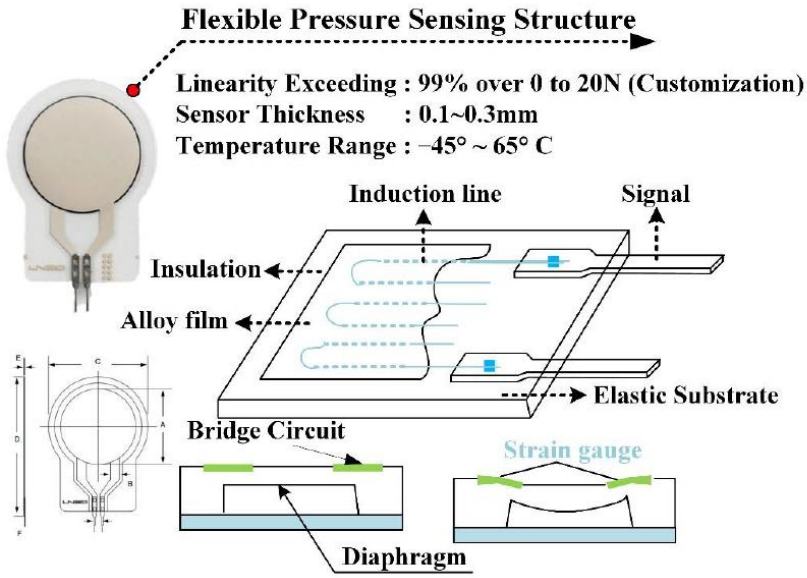

Figure 5. Structural representation of the flexible thin film pressure sensor.

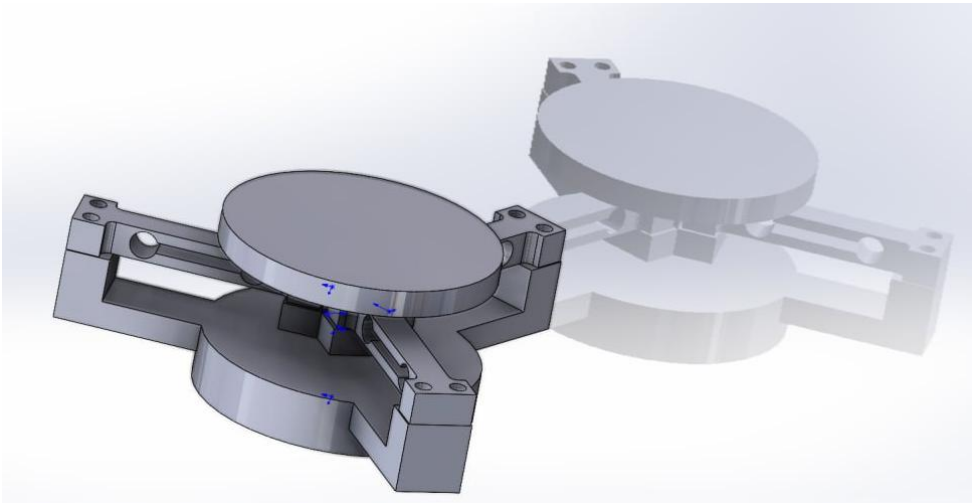

Figure 6. 3d model of sensor modul

In the course of production, the signal line was wrapped in the insulating layer to interference. As GD10-20N was produced using an imprinting and Flexible Printed Circuit (FPC) technique, the line spacing in the insulating layer was 0.1 mm. Thus, a precise circuit could be designed in a micro shape, and fabrication could be customized according to client-side requirements. GD10-20N, which was characterized by lightness, flexibility, and compactness, has good environment fitness, and remains sensitive at harsh ambient temperatures (−40°~65 °C). The output of sensors could be adjusted by an amplifier circuit to provide higher voltage range and the resolution. It
could increase the correlation between the output and the Newton force (0 N~20 N), which achieved the linearity of regressive analysis to 99%. The sensors could be reused ten million times. According to prior studies, the thin film pressure sensor has the advantages of system integration, as well as data linearity and reliability

Conclusion.

The researches were conducted on optimization of the ultrasound inspection path, on-site or remote control of the robot. But among open-source research, AI-based ra resource for conducting ultrasound examinations with the help of an obotit was not possible to find, therefore, research in this direction can make it possible to create a new type of robotic ultrasound system. In order to obtain the external actual contact force of the probe, the raw data of the force sensor are gravity compensated. The final value theorem is used to obtain the conditions under which the contact force reaches the desired force; that is, the suitable reference trajectory is required. In order to solve the problem of force tracking control under the condition of insufficient or unknown environmental information, this paper designs an adaptive control strategy from the perspective of real-time estimation of the environmental position and stiffness so as to predict and generate the subsequent reference trajectory points. Subsequently, the convergence proof of the proposed control strategy is provided in conjunction with the Lyapunov stability theory. In addition, in order to improve the system's ability to handle complex environments, an integral controller is introduced, and the boundary conditions are obtained by combining the Routh criterion. Finally, through the final value theorem, the validity of the introduced integral controller is proven.

Through simulation experiments of three control strategies in different scenarios, it is proven that IAAC can achieve the fast and compliant adjustment of the contact force. The results show that the force overshoot is significantly reduced, and the force tracking mean square error is the smallest in IAAC compared to AC. Finally, the experiments are carried out on the robotic ultrasonic scanning system. The results show that the force overshot of IAAC is reduced by 69.2%, and the steady-state force fluctuation range is reduced by 55.6% compared with AC on the flat skin surface. On the kidney and heart models, the force overshooting values of IAAC are 8.3% and 2.6% of the desired force, respectively, and high force tracking accuracy is maintained. In conclusion, the proposed strategy can significantly improve the force control performance of a robotic US system in a soft uncertain environment. This is a promising and meaningful study because it shows that the proposed system can partially play the role of a sonographer and act as a medical assistant to reduce the workload. Future work should consider the influence of patient

motions, such as breathing and heartbeats, and consider the ultrasound image quality as one of the control objectives to improve the applicability of the control strategy further.

References:

1. Current applications of robot-assisted ultrasound examination. Edgar m. Hidalgo bs a, leah wright phd b, mats isaksson phd a, gavin lambert phd ac, thomas h. Marwick mbbs, phd, mph bvolume 16, issue 2, February 2023, pages 239-247
2. A novel ultrasound robot with force/torque measurement and control for safe and efficient scanning,xianqiang bao,10.1109/tim.2023.3239925
3. Burke, M., Lu, K., Angelov, D., Straizys, A., Innes, C., Subr, K., Ramamoorthy,
4. S., 2020. Learning robotic ultrasound scanning using probabilistic temporal ranking. arXiv preprint arXiv:2002.01240 .
5. Merouche, S., Allard, L., Montagnon, E., Soulez, G., Bigras, P., Cloutier, G., 2015. A robotic ultrasound scanner for automatic vessel tracking and three-dimensional reconstruction of b-mode images. IEEE transactions on ultrasonics, ferroelectrics, and frequency control 63, 35–46.
6. Chan, V.; Perlas, A. Basics of ultrasound imaging. In Atlas of Ultrasound-Guided Procedures in Interventional Pain Management; Narouze, S.N., Ed.; Springer: New York, NY, USA, 2011; pp. 13–19. ISBN 978-1-4939-7752-9. [**Google Scholar**]
7. Harrison, G.; Harris, A. Work-related musculoskeletal disorders in ultrasound: Can you reduce risk? Ultrasound **2015**, 23, 224–230. [**Google Scholar**] [**CrossRef**]
8. Barr, R.G.; Zhang, Z. Effects of precompression on elasticity imaging of the breast: Development of a clinically useful semiquantitative method of precompression assessment. J. Ultrasound Med. **2012**, 31, 895–902. [**Google Scholar**] [**CrossRef**] [**PubMed**]
9. Tan, J.; Li, Y.; Li, B.; Leng, Y.; Peng, J.; Wu, J.; Luo, B.; Chen, X.; Rong, Y.; Fu, C. Automatic Generation of Autonomous Ultrasound Scanning Trajectory Based on 3-D Point Cloud. IEEE Trans. Med. Robot. **2022**, 4, 976–990. [**Google Scholar**] [**CrossRef**]
10. Holzgrefe, R.E.; Wagner, E.R.; Singer, A.D.; Daly, C.A. Imaging of the peripheral nerve: Concepts and future direction of magnetic resonance neurography and ultrasound. J. Hand. Surg. Am. **2019**, 44, 1066–1079. [**Google Scholar**] [**CrossRef**]
11. Priester, A.M.; Natarajan, S.; Culjat, M.O. Robotic ultrasound systems in medicine. IEEE Trans. Ultrason. Ferroelectr. Freq. Control **2013**, 60, 507–523. [**Google Scholar**] [**CrossRef**] [**PubMed**]
12. Huang, Q.; Lan, J. Remote control of a robotic prosthesis arm with six-degree-of-freedom for ultrasonic scanning and three-dimensional imaging. Biomed. Signal Process. Control **2019**, 54, 101606. [**Google Scholar**] [**CrossRef**]
13. Sartori, E.; Tadiello, C.; Secchi, C.; Muradore, R. Tele-echography using a two-layer teleoperation algorithm with energy scaling. In Proceedings of the 2019 International Conference on Robotics and Automation (ICRA), Montreal, QC, Canada, 20–24 May 2019; pp. 1569–1575. [**Google Scholar**]
14. Salcudean, S.E.; Moradi, H.; Black, D.G.; Navab, N. Robot-assisted medical imaging: A review. Proc. IEEE Inst. Electr. Electron. Eng. **2022**, 110, 951–967. [**Google Scholar**] [**CrossRef**]
15. Jiang, Z.; Grimm, M.; Zhou, M.; Hu, Y.; Esteban, J.; Navab, N. Automatic force-based probe positioning for precise robotic ultrasound acquisition. IEEE Trans. Ind. Electron. **2021**, 68, 11200–11211. [**Google Scholar**] [**CrossRef**]